B-12

Allosteric ClpP Agonist JZP3507 (ONC206) Alters Mitochondrial Metabolism, Stress Response, and Chromatin Accessibility to Elicit Apoptosis in Pheochromocytoma

Cristina Maranto, Scott Foster, Andrew Lee, Varun V. Prabhu*, Joshua E. Allen

Chimerix, Inc. (a Jazz Pharmaceuticals company), Durham, NC, USA

*Presenting author: Varun V. Prabhu

Objective

- To assess the mechanism of action of JZP3507 (formerly ONC206) in pheochromocytoma cells lines

Conclusions

- JZP3507 exhibits enhanced nanomolar potency and superior apoptosis relative to dordaviprone, temozolomide, sunitinib, and belzutifan in phecromocytoma (PC) cell lines
- The mitochondrial protease caseinolytic mitochondrial matrix peptidase proteolytic subunit (ClpP) expression and agonism are key for the anticancer efficacy of JZP3507 in vitro
- JZP3507 treatment is associated with alterations in mitochondrial metabolism, caseinolytic mitochondrial matrix peptidase chaperone subunit X, chromatin accessibility, stress response, neuroendocrine markers, and cell cycle in PC cells
- ClpP mediates response and acquired resistance to JZP3507 in PC cells

References: 1. Allen JE, et al. *Sci Transl Med.* 2013;5(171):171ra17. **2.** Free RB, et al. *Mol Pharmacol.* 2021;100(4):372-87. **3.** Madhukar NS, et al. *Nat Commun.* 2019;10(1):5221. **4.** Ishizawa J, et al. *Cancer Cell.* 2019;35(5):721-37.e9. **5.** Graves PR, et al. *ACS Chem Biol.* 2019;14(5):1020-9. **6.** Arrillaga-Romany I, et al. *J Clin Oncol.* 2024;42:1542-52. **7.** Theeler BJ, et al. *J Clin Oncol.* 2020;38(suppl 15):TPS2576. **8.** Jazz Pharmaceuticals. Study of ONC206 (JZP3507) in advanced pheochromocytoma and paraganglioma. ClinicalTrials.gov. June 10, 2026. Accessed September 22, 2026. https://clinicaltrials.gov/study/NCT07282587. **9.** Wagner J, et al. *Cell Cycle.* 2017;16(19):1790-9. **10.** Staley A, et al. *Am J Cancer Res.* 2021;11(11):5374-87. **11.** Zhang Y, et al. *Front Oncol.* 2020;10:577141. **12.** Tucker K, et al. *Am J Cancer Res.* 2022;12(2):521-36. **13.** Prabhu VV, et al. *Cancer Res.* 2020;80 (suppl 16):5688.

Support and Acknowledgments: This research was funded by Jazz Pharmaceuticals. Under the direction of the authors, Marita Chakhtoura, MS, PhD, CMPP, of Red Nucleus, provided medical writing and editorial support, which were funded by Jazz Pharmaceuticals in accordance with Good Publication Practice (GPP 2022) guidelines (https://www.ismpp.org/gpp-2022). Jazz Pharmaceuticals also reviewed and edited the poster for scientific accuracy.

Disclosures: CM, SF, AL, VVP, and JEA are employees of and have stock ownership in Jazz Pharmaceuticals. **VVP** and **JEA** are shareholders of Oncoceutics, Inc.

Corresponding author: Joshua E. Allen, PhD; Joshua.Allen@jazzpharma.com

Presented at the North American Neuroendocrine Tumor Society (NANETS) Annual Meeting; Las Vegas, NV; November 5–7, 2026

These data were originally presented at the 2025 North American Neuroendocrine Tumor Society (NANETS); October 23–25, 2025; Austin, TX. Abstract #9-10.

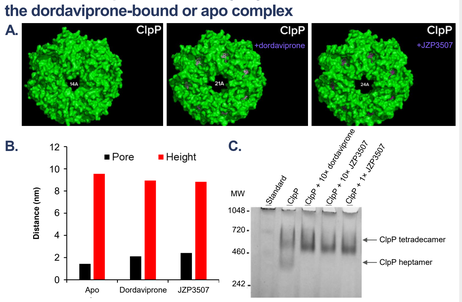
Copies of this poster obtained through the QR code are for personal use only and may not be reproduced without permission from the authors.

Introduction

- Dordaviprone, a first-in-class imipridone, is an oral, blood-brain barrier–penetrating, selective small molecule antagonist of dopamine receptor D2 (DRD2) and an agonist of the mitochondrial protease ClpP[1-5]
- Dordaviprone is approved by the US Food and Drug Administration for the treatment of adult and pediatric patients with H3 K27M-mutant diffuse midline glioma and has demonstrated tolerability and durable tumor regression in patients with H3 K27M-mutant glioma[6]
- JZP3507, an oral, central nervous system–penetrant, second-generation imipridone,[7] is the second imipridone to be developed and is in phase 2 clinical development[8]
- Relative to dordaviprone, JZP3507 has demonstrated differentiated DRD2 receptor pharmacology,[9] improved potency, enhanced absorption/tissue distribution, and preclinical anticancer activity in vitro and in vivo[9-13]

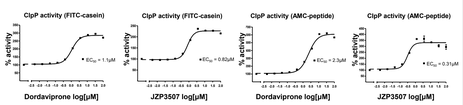
Results

Figure 1. Cocrystallization with ClpP revealed distinctions in the JZP3507-ClpP resolved X-ray crystal structure relative to the dordaviprone-bound or apo complex



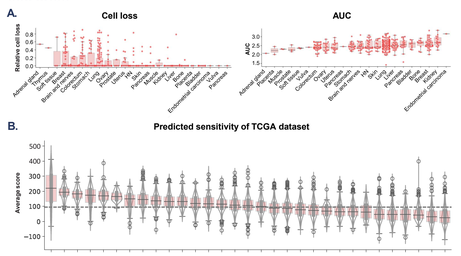
A. X-ray ClpP crystal structures for data shown in B with indicated pore size. **B**. Resolved pore size and complex height (nm) for ClpP apo or dordaviprone-bound or JZP3507-bound complex. **C**. Native gel analysis for ClpP with/without 1× or 10× molar concentration of dordaviprone or JZP3507. Apo, apoprotein; ClpP, caseinolytic mitochondrial matrix peptidase proteolytic subunit; MW, molecular weight (kDa).

Figure 2. JZP3507 exhibits enhanced nanomolar potency relative to dordaviprone in cell-free proteolysis assays



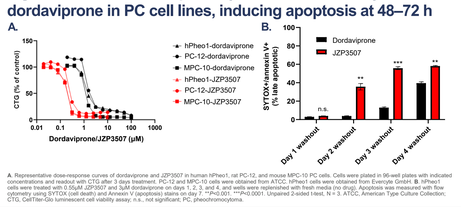
Wild-type ClpP protein was expressed in vitro, purified by His-affinity, and assayed for activity using FITC-casein and AMC peptide substrates as described previously.[4] AMC, 7-amino-4-methylcoumarin; ClpP, caseinolytic mitochondrial matrix peptidase proteolytic subunit; EC_{50}, half maximal effective concentration; FITC, fluorescein isothiocyanate.

Figure 3. Adrenal gland tumors emerge as most sensitive to JZP3507 when assessed in a panel of 432 human cancer cell lines



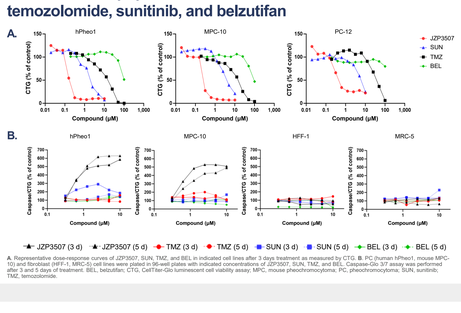
A. Cell loss and AUC of JZP3507 were evaluated in a CyQuant assay across various solid tumor lineages. Cytotoxicity is selective for specific tumor lineages, with strongest effects in adrenal gland, thymus, soft tissue, breast, and brain and nerve cell lines. Y-axis shows relative cell loss, x-axis cell lines grouped by lineage. **B**. Violin plot of the ranked TCGA lineages. Ranked in ascending order according to predicted sensitivity via cell panel-derived gene signature. The y-axis represents the average score predicted by the gene signature. AUC, area under the curve; TCGA, The Cancer Genome Atlas Program.

Figure 4. JZP3507 more potently inhibits cell viability than dordaviprone in PC cell lines, inducing apoptosis at 48–72 h



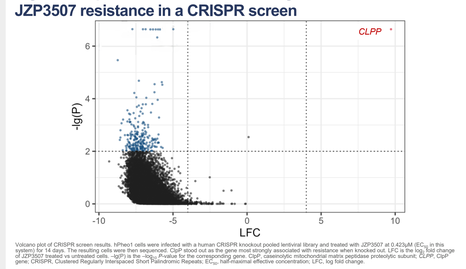
A. Representative dose-response curves of dordaviprone and JZP3507 in human hPheo1, rat PC-12, and mouse MPC-10 PC cells. Cells were plated in 96-well plates with indicated concentrations of dordaviprone or JZP3507 and readout with CTG (measures cell ATP content) after 5 days of treatment. ATP, adenosine triphosphate; CTG, CellTiter-Glo luminescent cell viability assay; KO, knockout; NTC, nontargeting control; PC, pheochromocytoma; WB, Western blot.

Figure 5. JZP3507 demonstrates superior cell viability inhibition and apoptosis in PC cell lines relative to temozolomide, sunitinib, and belzutifan



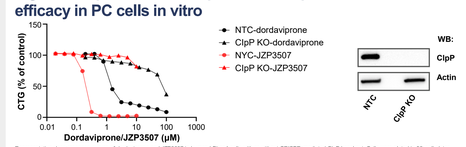
A. Representative dose-response curves of JZP3507, SUN, TMZ, and BEL in indicated cell lines after 3 days treatment as measured by CTG. **B**. PC (human hPheo1, mouse MPC-10) and fibroblast (HIFF-1, MRC-5) cell lines were plated in 96-well plates with indicated concentrations of JZP3507, SUN, TMZ, and BEL. Caspase-Glo 3/7 assay was performed after 3 and 5 days of treatment. BEL, belzutifan; CTG, CellTiter-Glo luminescent cell viability assay; MPC, mouse pheochromocytoma; PC, pheochromocytoma; SUN, sunitinib; TMZ, temozolomide.

Figure 6. ClpP knockout had the strongest association with JZP3507 resistance in a CRISPR screen



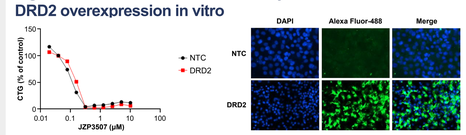
Volcano plot of CRISPR screen results. hPheo1 cells were infected with a human CRISPR knockout pooled lentiviral library and treated with JZP3507 at 0.425µM (EC_{50} in this system) for 14 days. The resulting cells were then sequenced. ClpP stood out as the gene most strongly associated with resistance when knocked out. LFC is the log_2 fold change of JZP3507 treated cells relative to control cells. The x-axis is the average LFC for each gene. CRISPR, Clustered Regularly Interspaced Short Palindromic Repeats; mitochondrial matrix peptidase proteolytic subunit; CLPP, ClpP gene; CRISPR, Clustered Regularly Interspaced Short Palindromic Repeats; EC_{50}, half-maximal effective concentration; LFC, log fold change.

Figure 7. ClpP knockout impairs dordaviprone and JZP3507 efficacy in PC cells in vitro



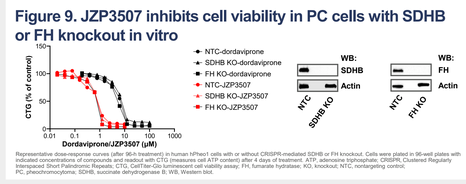
Representative dose-response curves of dordaviprone and JZP3507 in human hPheo1 cells with or without CRISPR-mediated ClpP knockout. Cells were plated in 96-well plates with indicated concentrations of JZP3507 and readout with CTG (measures cell ATP content) after 5 days of treatment. ATP, adenosine triphosphate; ClpP, caseinolytic mitochondrial matrix peptidase proteolytic subunit; CRISPR, Clustered Regularly Interspaced Short Palindromic Repeats; CTG, CellTiter-Glo luminescent cell viability assay; KO, knockout; NTC, nontargeting control; PC, pheochromocytoma; WB, Western blot.

Figure 8. JZP3507 inhibits cell viability in PC cells with DRD2 overexpression in vitro



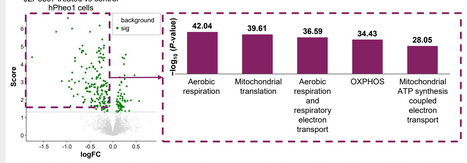
Representative dose-response curves of JZP3507 (after 96-h treatment) in human hPheo1 cells with or without DRD2 overexpression. Cells were plated in 96-well plates with indicated concentrations of JZP3507 and readout with CTG (measures cell ATP content) after 4 days of treatment. Immunofluorescence staining in hPheo1-NTC and DRD2 overexpression cell lines. ATP, adenosine triphosphate; CTG, CellTiter-Glo luminescent cell viability assay; DAPI, 4',6-diamidino-2-phenylindole; DRD2, dopamine D2 receptor; NTC, nontargeting control; PC, pheochromocytoma.

Figure 9. JZP3507 inhibits cell viability in PC cells with SDHB or FH knockout in vitro



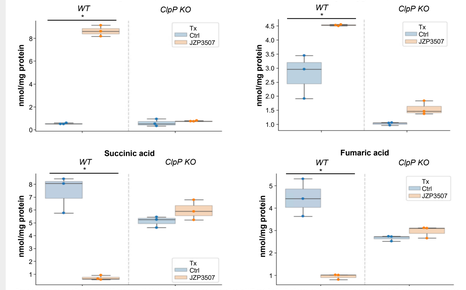
Representative dose-response curves (after 96-h treatment) in human hPheo1 cells with or without CRISPR-mediated SDHB or FH knockout. Cells were plated in 96-well plates with indicated concentrations of compounds and readout with CTG (measures cell ATP content) after 4 days of treatment. ATP, adenosine triphosphate; CRISPR, Clustered Regularly Interspaced Short Palindromic Repeats; CTG, CellTiter-Glo luminescent cell viability assay; FH, fumarate hydratase; KO, knockout; NTC, nontargeting control; PC, pheochromocytoma; SDHB, succinate dehydrogenase B; WB, Western blot.

Figure 10. Proteomics indicates JZP3507 alters mitochondrial proteins in hPheo1 cells, including OXPHOS and TCA cycle



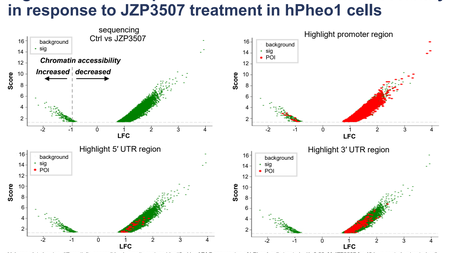
Volcano plot showing differentially abundant proteins between JZP3507-treated (0.05µM, 24 h) and control hPheo1 cells. Green dots represent proteins with a false discovery rate below 5%. Score: $-log_{10}$(adjusted P-value); logFC: log_2(JZP3507/ctrl). Overrepresentation analysis (bar chart) of depleted proteins, highlighting the most significantly enriched biologic terms. ATP, adenosine triphosphate; ctrl, control; FC, fold change; OXPHOS, oxidative phosphorylation; sig, signal; TCA, tricarboxylic cycle.

Figure 11. Metabolomics reveals JZP3507 elevated α-ketoglutaric acid, 2-hydroxyglutaric acid and reduced succinic acid, fumaric acid in a ClpP-dependent manner in hPheo1 cells



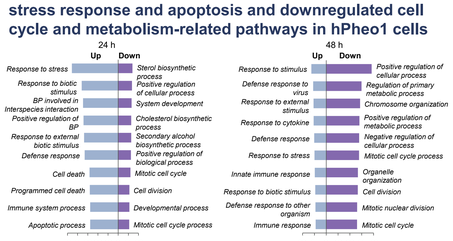
Box plots showing the effect of JZP3507 treatment (0.05µM, 48 h) on selected metabolites in WT and ClpP KO hPheo1 cells. *P<0.05 (Welch's t-test). ClpP, caseinolytic mitochondrial matrix peptidase proteolytic subunit; ctrl, control; KO, knockout; Tx, treatment; WT, wild-type.

Figure 12. ATACseq shows altered chromatin accessibility in response to JZP3507 treatment in hPheo1 cells



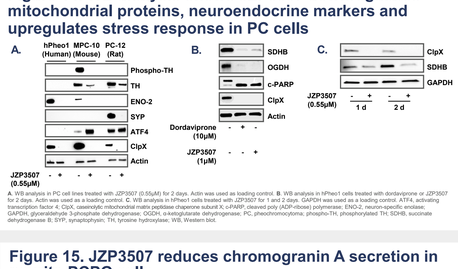
Volcano plot showing differentially accessible chromatin regions identified by ATAC sequencing of hPheo1 cells treated with 0.55µM JZP3507 for 48 h vs control untreated cells. Green dots represent regions with a false discovery rate below 5%. Score: $-log_{10}$(P-value); LFC: log_2(ctrl/JZP3507). ATAC, assay for transposase-accessible chromatin; ATACseq, ATAC with high-throughput sequencing; ctrl, control; LFC, log fold change; POI, protein of interest; sig, signal; UTR, untranslated region.

Figure 13. RNAseq demonstrates JZP3507 upregulated stress response and apoptosis and downregulated cell cycle and metabolism-related pathways in hPheo1 cells



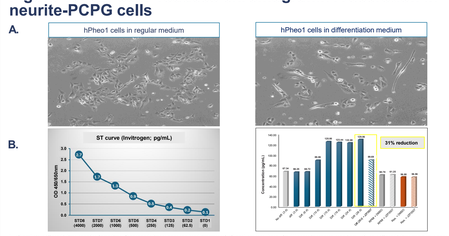
Overrepresentation analysis of biologic processes enriched or depleted (false discovery rate <5%) in significantly altered mRNAs following JZP3507 (0.55µM) treatment of hPheo1 cells. Panels show the most significantly enriched terms at 24 and 48 h post-treatment. BP, biologic process; RNAseq, RNA sequencing.

Figure 14. WB analysis shows JZP3507 downregulates mitochondrial proteins, neuroendocrine markers and upregulates stress response in PC cells



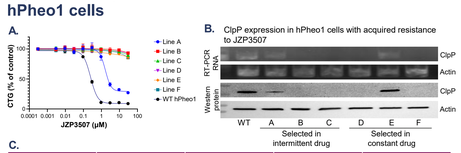
A. WB analysis in PC cell lines treated with JZP3507 (0.55µM) for 2 days. Actin was used as loading control. **B**. WB analysis in hPheo1 cells treated with dordaviprone or JZP3507 for 2 days. Actin was used as a loading control. **C**. WB analysis in hPheo1 cells treated with JZP3507 for 1 and 2 days. GAPDH was used as a loading control. ATF4, activating transcription factor 4; ClpX, caseinolytic mitochondrial matrix peptidase chaperone subunit X; c-PARP, cleaved poly (ADP-ribose) polymerase; ENO-2, neuron-specific enolase; GAPDH, glyceraldehyde 3-phosphate dehydrogenase; OGDH, α-ketoglutarate dehydrogenase; PC, pheochromocytoma; phospho-TH, phosphorylated TH; SDHB, succinate dehydrogenase B; SYP, synaptophysin; TH, tyrosine hydroxylase; WB, Western blot.

Figure 15. JZP3507 reduces chromogranin A secretion in neurite-PCPG cells



A. hPheo1 cell differentiation–neurite formation. Representative phase-contrast images of hPheo1 cells cultured for 19 days in regular medium (left) or differentiation medium (bone morphogenetic protein-4, dexamethasone, and nerve growth factor; right). **B**. Effect of JZP3507 on secreted chromogranin A in neurite-PCPG cells by ELISA. Neurite-PCPG cells were treated with JZP3507 for 19 days in differentiation medium. Chromogranin A was measured in the conditioned medium of hPheo1 and JZP3507-resistant cell lines compared with undifferentiated cells and JZP3507-resistant cell lines. bFGF, basic fibroblast growth factor; BMP-4, bone morphogenetic protein-4; CGNT, catechol-O-methyltransferase; Dex, dexamethasone; diff., differentiation; DMEM/F12, Dulbecco's Modified Eagle Medium F12; DMSO, dimethyl sulfoxide; EGF, epidermal growth factor; ELISA, enzyme-linked immunosorbent assay; F12, Ham's factor 12; ITS, insulin transferrin; LIF, leukemia inhibitory factor; NGF, nerve growth factor; OD, optical density; PC, pheochromocytoma; PG, paraganglioma; Pheo1-Res, Pheo1-resistant; PNMT, phenyl ethanolamine N-methyltransferase; res., resistant; RPMI, Roswell Park Memorial Institute media; ST curve, standard curve; STD, standard; SYP, synaptophysin.

Figure 16. Acquired resistance to JZP3507 treatment in hPheo1 cells

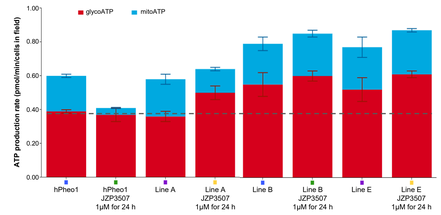


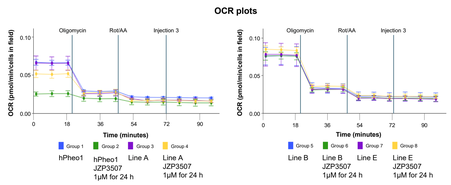
C.

Name	ClpP mutation	Mutant proportion	Mutation location	JZP3507 selection
Line A	Q134N	51.1%	Individual subunit interface	3 days on/4 days off
Line B	Q137X	51.1%	Termination	3 days on/4 days off
Line C	Q137X	99.1%	Termination	3 days on/4 days off
Line D	Q137X	98.8%	Termination	Continuous
Line E	Q137X G182E A195E	10.6% 20.7% 16.5%	Termination Heptamer interface Heptamer interface	Continuous
Line F	No mutation No mutation No mutation	Not applicable Not applicable Not applicable	No mutation No mutation No mutation	Continuous

A. Treatment to generate acquired resistance was initiated at 0.2µM JZP3507, and drug concentration was doubled when cells were able to proliferate. hPheo1 cells were selected up to 1.6µM JZP3507. Lines A, B, and C were selected under 3 days on/4 days off JZP3507 treatment. Lines D, E, and F were selected under constant JZP3507. Cell viability for 5000 cells treated with JZP3507 at indicated concentrations was measured on day 4 using CTG (Promega). **B**. RT-PCR and WB analysis for ClpP and actin expression in clones with acquired resistance to JZP3507 (1.6µM). Line A expresses ClpP RNA and protein (low protein compared to WT cells). Lines B and C ClpP RNA and protein were not detected. Line E expresses ClpP RNA and protein (comparable to WT cells). Lines D and F ClpP RNA and protein were not detected. **C**. Q137X is a termination. Whole-exome sequencing was performed at Nucleome. ATP, adenosine triphosphate; caseinolytic mitochondrial matrix peptidase proteolytic subunit; CTG, CellTiter-Glo luminescent cell viability assay; RT-PCR, reverse transcription polymerase chain reaction; WB, Western blot; WT, wild-type.

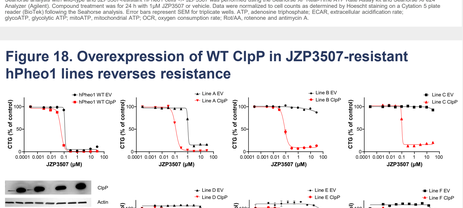
Figure 17. Seahorse analysis of hPheo1 cells with acquired resistance to JZP3507 reveals impaired effects on glyco and mito ATP compared to parental cells





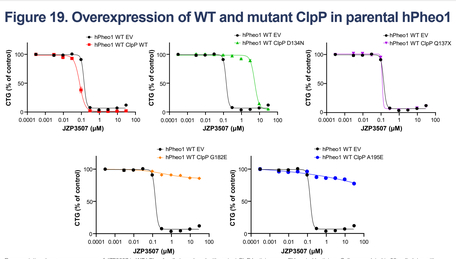
Seahorse analysis with wild-type and JZP3507-resistant hPheo1 cells +/- JZP3507 was performed using the Seahorse XF Real-Time ATP Rate Assay kit and Seahorse XFe24 Analyzer (Agilent). Compound treatment was for 24 h with 1µM JZP3507 or vehicle. Data were normalized to cell counts as determined by Hoescht staining on a Cytation 5 plate reader (BioTek) following the Seahorse analysis. Error bars represent SEM for triplicate wells. ATP, adenosine triphosphate; ECAR, extracellular acidification rate; glycoATP, glycolytic ATP; mitoATP, mitochondrial ATP; OCR, oxygen consumption rate; Rot/AA, rotenone and antimycin A.

Figure 18. Overexpression of WT ClpP in JZP3507-resistant hPheo1 lines reverses resistance



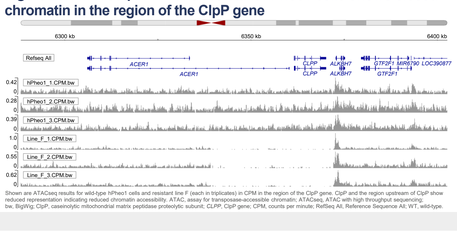
Representative dose-response curves of JZP3507 in WT hPheo1 cells and JZP3507-resistant derivatives transduced with WT ClpP overexpression lentivirus (ClpP) or EV control lentivirus. Cells were plated in 96-well plates with indicated concentrations of JZP3507 and readout with CTG (measures cell ATP content) after 4 days of treatment. Inset shows WB for ClpP and actin to demonstrate overexpression. ATP, adenosine triphosphate; ClpP, caseinolytic mitochondrial matrix peptidase proteolytic subunit; CTG, CellTiter-Glo luminescent cell viability assay; EV, empty vector; WB, Western blot; WT, wild-type.

Figure 19. Overexpression of WT and mutant ClpP in parental hPheo1



Representative dose-response curves of JZP3507 in WT hPheo1 cells transduced with mutant ClpP lentivirus or EV control lentivirus. Cells were plated in 96-well plates with indicated concentrations of JZP3507 and readout with CTG (measures cell ATP content) after 4 days treatment. Q137X is a termination mutation and is not expected to express protein. ATP, adenosine triphosphate; ClpP, caseinolytic mitochondrial matrix peptidase proteolytic subunit; CTG, CellTiter-Glo luminescent cell viability assay; EV, empty vector; WT, wild-type.

Figure 20. ATACseq in WT and resistant hPheo1 cells shows closed chromatin in the region of the ClpP gene



Shown are ATACseq results for wild-type hPheo1 cells and resistant line F (each in triplicates) in CPM in the region of the ClpP gene. ClpP and the region upstream of ClpP show reduced repressed representation indicating reduced chromatin accessibility. ATAC, assay for transposase-accessible chromatin; ATACseq, ATAC with high throughput sequencing; bw, BigWig; ClpP, caseinolytic mitochondrial matrix peptidase proteolytic subunit; CLPP, ClpP gene; CPM, counts per minute; RefSeq All, Reference Sequence All; WT, wild-type.